

Basic Principles of Wave Optics

Basic optometric education has emphasized geometric rather than wave optics, and this has been sufficient to prepare optometrists for the majority of optics problems they encounter in clinical practice. Geometric optics uses ray propagation to describe light, and clinical problems can usually be solved with its straightforward paraxial equations. The increasing importance of optical aberrations in vision research and in clinical practice requires that modern optometrists have a more thorough understanding of the wave properties of light. Chapter 2 reviews basic principles that were used in the experimental design, data analysis and interpretation of data in this research.

2.1

OPTICAL PATH LENGTH

Light propagates through space in the form of waves, somewhat like the ripples created when a stone is dropped in a pond. The pond ripples are formed as crests and troughs, expanding outward, and when seen from above, they look like expanding circles. Since all portions of the wavefront propagate through water with uniform velocity, all points on this circle are equidistant from the center, and all points will have been traveling for the same length of time. Similarly, for a pulse of light emitted from a point source in three-dimensional space, the wavefronts are like expanding spherical shells. At any instant, all points on a wavefront will be equidistant from the point source, and each point will have traveled for equal time. The wavefront expands very quickly since the waves propagate through space at the speed of light.

The velocity of light in a vacuum (v_0) is constant for all wavelengths but it is slower in other optical media, and the velocity will vary as a function of wavelength (λ). The refractive index (n) of a medium is defined for each wavelength as the ratio of the velocity of light in a vacuum to the velocity (v_m) of that wavelength in the medium (Eq. 2-1). A wavelength of 589 nm is commonly used as the reference wavelength when specifying the index of refraction for optical materials.

$$n = \frac{v_0}{v_m} \quad (2-1)$$

Frequency (f) is inversely proportional to wavelength (Eq. 2-2), and for a particular wavelength, its frequency remains constant in all optical media. In order for the frequency to remain constant, the wave-

$$f = \frac{v}{\lambda} \quad (2-2)$$

length in a new medium (λ_m) must change in proportion to its velocity (v_m) in that medium. For example, when crossing from air to a denser medium, velocity decreases and the wavelength also decreases. As a consequence, the wavelength of light in a new medium is equal to the wavelength in a vacuum (λ_0) divided by the index of refraction:

$$f = \frac{v_0}{\lambda_0} = \frac{v_m}{\lambda_m} \text{ therefore, } \frac{v_0}{v_m} = \frac{\lambda_m}{\lambda_0} = n, \text{ and } \lambda_m = \frac{\lambda_0}{n} \quad (2-3)$$

In some cases it is necessary to calculate the physical distance traveled by light in a new medium, and the relationship is developed in Eq. (2-4). The physical distance traveled by light in a vacuum in unit time (t) is d_0 , so the physical distance traveled in another medium (d_m) during the same time is the distance in a vacuum divided by the medium's index of refraction.

$$\frac{d_m}{t} = v_m = \frac{v_0}{n} = \frac{\left(\frac{d_0}{t}\right)}{n}, \text{ therefore, } d_m = \frac{d_0}{n} \quad (2-4)$$

In some cases the distance traveled by light in a medium is known (d_m), but we must calculate the distance it would have traveled in a vacuum (d_0) during the same time. This is known as the optical path

length (OPL), and it can be expressed in units such as micrometers. Equation (2-5), which is equivalent to Eq. (2-4), shows that the OPL is the product of distance d_m and the refractive index (n) of that medium.

$$OPL = d_m n \tag{2-5}$$

The distance traveled by light in any media may also be normalized by the wavelength in that medium (λ_m). As shown in Eq. (2-6), this is equal to the OPL divided by the wavelength in a vacuum. Since image formation and image quality depend on interference of wavefronts, it is useful to describe OPL errors, that is aberrations, in terms of wavelengths.

$$\frac{d_m}{\lambda_m} = \frac{d_m}{\left(\frac{\lambda}{n}\right)} = \frac{d_m n}{\lambda} = \frac{OPL}{\lambda} \tag{2-6}$$

2.2

WAVEFRONT ABERRATION

For light entering a theoretically perfect (defocus, aberration and diffraction free) eye, refracted light, after passing through the exit pupil, converges in the form of spherical wavefronts to a focal point on the retina. Recalling that an optical wavefront represents a surface of uniform distance and time traveled, all points on the wavefront are in phase. Therefore when the spherical wavefront collapses to the focal point, all the light arrives at this point in phase, and maximum radiant energy is delivered to that point (Williams & Becklund, 1989). If there were no diffraction (physically impossible), this would form a perfect point, but because of diffraction, even the most perfect optical system will form a focal point that is slightly blurred. For a round pupil, the diffraction pattern of a point source appears as a bright spot, the *Airy disk* (Fig. 2.1), surrounded by faint concentric rings. The angular width of the Airy disk in radians (θ) may be calculated for a circular aperture by Eq. (2-7), where the diameter (p) and wavelength (λ) are in meters.

$$\theta = \frac{2.44 \lambda}{p} \tag{2-7}$$

In the case of a square aperture, a factor of 2 rather than 2.44 is used. If the focal length is known, the

linear extent (s) of the Airy disk can be calculated from Eq. (2-8), where $f/\#$ is the ratio of focal length to aperture diameter.

$$= \frac{2.44}{p} = \frac{s}{f}, \text{ therefore, } s = \frac{2.44 f}{p} = 2.44 (f/\#) \quad (2-8)$$

These basic formulae apply when the intensity distribution across the light beam is uniform. If the intensity is Gaussian, as is true for most laser beams, the focal point will not be an Airy disk, but will be a Gaussian spot, and the formula for estimating spot size becomes (Saleh & Teich,):

$$s = 4 (f/\#) \quad (2-9)$$

This formula (Eq. 2-9) may be used to estimate the spot size in Shack-Hartmann wavefront sensor reference images.

Diffraction is a fundamental property of the wave nature of light whenever it passes through an aperture. Since all optical systems have a limiting aperture, it is impossible to build a diffraction-free optical device. It is possible, by careful design, to improve image quality in an optical system by reducing aberrations, but it is impossible to exceed the limits to image quality set by diffraction. Ultimate optical quality is therefore referred to as “diffraction limited”—that is, limited by diffraction only.

Light passing through an optical system, which is less than perfect, will produce a wavefront in the exit pupil that is aberrated from the ideal spherical surface, known as the *pupil sphere*. The apex of the pupil sphere coincides with the pupil center (Fig 2.2 point p), and its center of curvature is the paraxial focal point (f). Except in the case of very small pupils, where diffraction is large, aberrations are usually the major factor beyond defocus that degrades image quality. The wavefront aberration function, $W(x,y)$, is the scalar distance between the aberrated wavefront and the pupil sphere. Its precise definition varies slightly in different optics reference books. For the refracted ray (heavy line) shown in Fig. 2.2, the wavefront aberration at point a is defined as distance ab (Hopkins, 1950; Born & Wolf, 1980), or it may be defined at point a' as distance $a'b$ (Williams & Becklund, 1989; Smith, 1990). For the range of typical ocular wavefront aberrations, these distances are essentially equal (Welford, 1986). For points on the aberrated wavefront that have advanced ahead of the pupil sphere, the sign of $W(x,y)$ is positive. For portions of the wavefront that are retarded behind the pupil sphere, the sign is negative. The physical distance between the wavefront and pupil sphere is usually multiplied by the index of refraction (for OPL), divided by the wavelength in a vacuum (yields number of wavelengths), and multiplied by 2, to transform

the distance into a phase error. The wavefront aberration is the most important component of the *pupil function*, $P(x,y)$ shown in Eq. (2-10), which "incorporates complete information about the imaging properties of the optical system" (Williams & Becklund, 1989).

$$P(x,y) = A(x,y)e^{-i2\pi W(x,y)/\lambda} \quad (2-10)$$

In this equation, $A(x,y)$ is an amplitude function describing the relative efficiency of light passing through the pupil, and is usually given a uniform value of 1.0. In cases where the Stiles-Crawford effect is taken into account, it can be included here (van Meeteren, 1974). Once the aperture function is known, the principles of Fourier optics may be employed to compute the optical transfer function (OTF) and point spread function (PSF) which describe the imaging performance of the system. The surface plot in Fig. 2.3 represents a theoretical wavefront aberration function $W(x,y)$, for a cornea which has both astigmatism and spherical aberration. Wavefront aberration functions are usually sampled at many discrete locations within the pupil, and it may be summarized by a single numerical value such as the wavefront variance or root mean squared (RMS) wavefront error.

2.3

FOURIER OPTICS

Fourier optics is a powerful tool for analyzing and manipulating the optical transfer function (Thibos, 1993; Goodman, 1996). The optical transfer function (OTF) is one of the most useful descriptors of imaging performance for an optical system. It is a complex number whose magnitude is the modulation transfer function (MTF), and the phase is the phase transfer function (PTF). The MTF plots the relative contrast reduction between object and image as a function of spatial frequency, while the phase transfer function describes the lateral image shift as a function of spatial frequency. If the wavefront aberration function, $W(x,y)$ is known, the pupil function, $P(x,y)$, can be calculated (Eq. 2-10), and from this, the OTF may be computed by convolving the pupil function with its complex conjugate, $P^*(-x,-y)$, as shown in Eq. (2.11). The \otimes symbol represents convolution.

$$OTF(f_x, f_y) = P(x,y) \otimes P^*(-x,-y) \quad (2-11)$$

This is the same as taking the autocorrelation of the pupil function. By the convolution theorem, the parallel operation can be performed in the frequency domain by multiplication. Therefore, the Fourier transform (F) of the OTF is the product the Fourier transforms of the pupil function and its complex conjugate:

$$F[\text{OTF}(f_x, f_y)] = F[P(x, y)] \times F[P^*(-x, -y)] \quad (2-12)$$

The point spread function (PSF), another important measure of image quality, is the image of a point source formed by the optical system. In the case of a diffraction limited (no aberrations) system, the PSF is the Airy disk. Aberrations will cause additional spreading or blurring of the point. The Strehl ratio is sometimes used to describe image quality of a well corrected system, and it is defined as the maximum intensity of the PSF divided by the theoretical diffraction limited maxima of the same system (Born & Wolf, 1980; Freeman, 1990). The Fourier transform of the OTF is the PSF, therefore all important metrics of image quality (MTF, PTF, PSF, and Strehl ratio) can be calculated from the OTF. The OTF for a system can be computed if the wavefront aberration is known. Examples of the MTF and PSF corresponding to the wavefront of Fig. 2.3 are shown in Figs. 2.4 and 2.5, respectively.

If any scene imaged by an optical system is considered a collection of points, the image of each point in the scene will be the PSF, and the integration of all the points will build the image of the scene formed by those optics. Mathematically, this is the convolution of the PSF with the scene, and is summarized by Eq. (2-13). $U(x, y)$ is the light intensity distribution of the perfect image that would be predicted by paraxial optics—that is, without aberrations or diffraction. $U'(x, y)$ is the light intensity for the image formed by the optical system. For large images, it may be easier to compute $U'(x, y)$ by multiplication in the frequency domain rather than by convolution in the spatial domain. Since the OTF is the Fourier transform of the PSF, the product of the $U(x, y)$ frequency spectrum and the OTF is the frequency spectrum, or Fourier transform, of the aberrated image (Eq. 2-14).

$$U'(x, y) = U(x, y) \otimes \text{PSF}(x, y) \quad (2-13)$$

$$F[U'(x, y)] = F[U(x, y)] \times \text{OTF}(f_x, f_y) \quad (2-14)$$

The aberrated image is then found by taking the inverse Fourier transform (F^{-1}) of this result:

$$U'(x, y) = F^{-1}\{F[U'(x, y)]\} \quad (2-15)$$

If the eye's PSF or OTF are known, it is theoretically possible to construct the image of any scene formed on the retina by convolution (Camp, Maguire, Cameron, & Robb, 1990) or Fourier multiplication. Figure 2.6 uses these principles to simulate the view of a mountain scene for an eye with astigmatism and

spherical aberration.

The reverse process can be used to recover the unaberrated image (the scene) from the aberrated image by deconvolution of the aberrated image by the PSF (Fig. 2.6). This is performed in the frequency domain (Russ, 1995) by dividing the aberrated image spectrum by the OTF (Eq. 2-16), and transforming the result to the spatial domain (Eq. 2-17). Division with complex numbers is accomplished by dividing the magnitudes and subtracting the phases.

$$F[U(x,y)] = \frac{F[U'(x,y)]}{\text{OTF}(f_x, f_y)} \quad (2-16)$$

$$U(x,y) = F^{-1}\{F[U(x,y)]\} \quad (2-17)$$

A practical application of this process is the recovery of unaberrated images of the retina taken through the aberrated optics of the eye by a retinal camera. Using deconvolution or the corresponding operations in the frequency domain, it is theoretically possible to recover high resolution images of the retina if the eye's OTF is known.

2.4

POLYNOMIAL EXPANSION OF ABERRATION FUNCTIONS

It is sometimes useful to trace light through an optical system by considering the path of a point on the wavefront. Within one optical medium, this point proceeds in a straight line (a ray) perpendicular to the wavefront but will change directions upon entering a new medium. This bending of light is refraction. Using Snell's law (Eq. 2-18) we can calculate the change of direction of the rays, and determine the location of the image point formed by different parts of the optical wavefront. Ray tracing can be used to study optical aberrations.

$$n_i \sin \theta_i = n_r \sin \theta_r \quad (2-18)$$

2.4.1 Taylor series expansion of the sine function

From the perspective of ray tracing, aberrations are present whenever a ray misses the ideal focal point (Fig. 2.2 point f) and may be expressed as a longitudinal distance along the optic axis or a transverse displacement of the ray above or below the focal point. Since the path of the light ray is proportional to the sine function, it is possible to analyze aberrations based on a Taylor series expansion (Freeman, 1990)

of the sine function:

$$\sin \theta = \theta - \frac{\theta^3}{3!} + \frac{\theta^5}{5!} - \frac{\theta^7}{7!} + \frac{\theta^9}{9!} - \dots \quad (2-19)$$

If the angle of incidence is very small, as when rays from a distant axial object strike the surface near the optic axis, $\sin \theta$ is closely approximated by the first term, θ , and all higher terms of the series may be ignored. Ray tracing with this paraxial approximation gives the location of an image point for an aberration free system, and is the basis for *Gaussian*, or *first order* optics. For larger angles of incidence, the second and higher terms of the series become increasingly important for describing the actual path of light. In this case, the rays depart increasingly from the paraxial prediction, and this departure from the path of the paraxial rays is an expression of the optical aberrations. The aberrations contained in the second term of the series are known as the *third order*, or primary aberrations; the next term contains the *fifth order*, or secondary aberrations, and so on. Most optics texts consider expansion as far as the third order sufficient to explain the most important optical aberrations. Ludwig von Seidel (1821-1896) studied the third order aberrations, and broke them down into five components, now known as the five monochromatic Seidel aberrations (spherical aberration, coma, astigmatism, Petzval curvature of field and distortion). Modern computers make it possible to accurately trace rays without these approximations, but analysis of aberrations into components, such as the Seidel aberrations, is still useful in studying the optics of a system.

2.4.2 Rotationally symmetric systems

Returning to the wavefront aberration, the wavefront surface may also be analyzed into components by expanding the function as a power series. For the relatively simple case of a rotationally symmetric system, one expansion of the wavefront aberration is shown in Eq. (2-20) (Williams & Becklund, 1989; Smith, 1990). This takes into account the distance of the object point from the optic axis (r) and expresses the pupil sphere coordinates (x,y) in polar terms, where ρ is the distance from the optic axis, and angle θ is measured from the vertical meridian. The coefficient C before each polynomial is subscripted with three numbers that indicate, from left to right, the power of the r , ρ , and $\cos \theta$ terms, respectively. The first three terms describe first order optics and include, in order, a constant, prism, and defocus. The next five terms (Eq. 2-20 second line) correspond to the third order Seidel aberrations, spherical aberration, coma, astigmatism, Petzval curvature and distortion. Addition of fifth order or higher terms will improve the polynomial approximation to the wavefront aberration, though the higher terms

normally account for a much smaller portion of the aberration. From this equation, we note that, for a point object located on the optic axis, the value for r is zero, and all Seidel aberrations except spherical aberration drop out.

$$W(r, \cos \theta) = {}_0C_{00} + {}_1C_{11}r \cos \theta + {}_0C_{20}r^2 + {}_0C_{40}r^4 + {}_1C_{31}r^3 \cos \theta + {}_2C_{20}r^2 \cos^2 \theta + {}_2C_{22}r^2 \cos^2 \theta + {}_3C_{11}r^3 \cos \theta + \dots \quad (2-20)$$

2.4.3 Asymmetric systems with axial objects

In contrast to most man made optical systems, the human eye is normally not rotationally symmetric, therefore asymmetric aberrations can arise even with an axial point source. Equation (2-21) is an aberration polynomial which includes this consideration and is sometimes used to analyze the wavefront aberration of the human eye (Howland & Howland, 1977) .

$$W(x,y) = A + Bx + Cy + Dx^2 + Exy + Fy^2 + Gx^3 + Hx^2y + Ixy^2 + Jy^3 + Kx^4 + Lx^3y + Mx^2y^2 + Nxy^3 + Oy^4 \dots \quad (2-21)$$

The terms associated with coefficients B and C represent horizontal and vertical prism; D, E and F are transforms of the spectacle sphere, cylinder and axis while, the K, M and O terms are components of third order spherical aberration.

2.4.4 Zernike polynomials

The Zernike polynomials have been used in optical engineering (Born & Wolf, 1980; Malacara & DeVore, 1992; Mahahan, 1994) for over 60 years, and recently these have been applied to aberrations of the human eye (Webb, 1992; Liang, Grimm, Goelz, & Bille, 1994; Liang & Williams, 1995) and corneal topography (Schwiegerling, Greivenkamp, & Miller, 1995; Schwiegerling, Greivenkamp, Miller, Snyder, & Palmer, 1996; Schwiegerling & Grievenkamp, 1996). This polynomial series offers the advantage of terms which are orthogonal for continuous curves, which is beneficial for surface fitting and analysis. Orthogonality cannot be assumed, however for discrete data or for nonuniform sampling (Wang & Silva, 1980). In some cases it may be necessary to perform a Gram-Schmidt orthogonalization to accurately apply Zernike polynomials (Schwiegerling, *et al.*, 1995). Either polar and Cartesian Zernike polynomials may be used, and depending on the reference, angles may be referenced to vertical or horizontal meridian. The

TABLE 2.1 A subset of the normalized Cartesian Zernike polynomials used in this dissertation.

Order	Mode	Polynomial	Description
0	1	1	piston
1	2	2y	vertical prism
1	3	2x	horizontal prism
2	4	6(2xy)	astigmatism axis 45/135
2	5	3(2x ² + 2y ² - 1)	defocus
2	6	6(x ² - y ²)	astigmatism axis 180/90
3	7	8(3x ² y - y ³)	triangular astigmatism
3	8	8(3x ² y + 3y ³ - 2y)	primary coma
3	9	8(3x ³ + 3xy ² - 2x)	primary coma
3	10	8(x ³ - 3xy ²)	triangular astigmatism
4	11	10(4x ³ y - 4xy ³)	
4	12	10(8x ³ y + 8xy ³ - 6xy)	
4	13	5(6x ⁴ + 12x ² y ² + 6y ⁴ - 6x ² - 6y ² + 1)	primary spherical
4	14	10(4x ⁴ - 3x ² + 3y ² - 4y ⁴)	
4	15	10(x ⁴ - 6x ² y ² + y ⁴)	
5	16	12(5x ⁴ y - 10x ² y ³ + y ⁵)	
5	17	12(15x ⁴ y - 12x ² y - 5y ⁵ + 4y ³ + 10x ² y ³)	
5	18	12(10x ⁴ y + 20x ² y ³ + 10y ⁵ - 12x ² y - 12y ³ + 3y)	secondary coma
5	19	12(10x ⁵ + 20x ³ y ² + 10xy ⁴ - 12x ³ - 12xy ² + 3x)	secondary coma
5	20	12(5x ⁵ - 10x ³ y ² - 4x ³ - 15xy ⁴ + 12xy ²)	
5	21	12(x ⁵ - 10x ³ y ² + 5xy ⁴)	

mode numbering scheme and order may also vary. Table 2.1 shows the Cartesian form of the first 21 Zernike modes, which I used. Note that the Zernike terms labeled primary coma or spherical aberration do not correspond directly with the Seidel aberrations of the same name. Zernike polynomials were used to analyze the corneal and ocular wavefront aberrations in this dissertation.

2.4.5 Converting Zernike second order polynomials to the equivalent ophthalmic spectacle prescription

The second Zernike order is made up of three modes, which are labeled 45/135 astigmatism (mode 4), defocus (mode 5) and 90/180 astigmatism (mode 6). They describe the optical defects that are corrected by conventional spectacles, namely myopia or hyperopia (defocus) and astigmatism. It is possible to convert this portion of the wavefront aberration to the equivalent ophthalmic spectacle prescription by the steps outlined below.

- 1) Compute the wavefront error (W) at the pupil edge, in meters, using Eq. (2-22) for mode 5 (defocus), Eq. (2-23) for mode 4 and Eq. (2-24) for mode 6 use.

$$W_5 = -a_5(2/3)(6.33 \times 10^{-7}) \quad (2-22)$$

$$W_4 = -a_4(6/6)(6.33 \times 10^{-7}) \quad (2-23)$$

$$W_6 = -a_6(6/6)(6.33 \times 10^{-7}) \quad (2-23)$$

Variable a , subscripted with the mode number, is the Zernike coefficient for the respective modes. A myopic wavefront error has a positive sign, but by clinical convention, myopic prescriptions are given a minus sign. Therefore all three equations include a minus sign. In my analysis, the Zernike coefficients described the wavefront errors in wavelengths, where one wavelength is 633 nm. The constant at the end of each equation converts the wavefront error in wavelengths to meters.

- 2) Strictly speaking the Zernike profiles are parabolic and a large number of parabolas must be summed to better approximate a circle. This would require that the higher order astigmatic modes contained in orders 4, 6, 8, and 10 also be included (Schwiegerling, *et al.*, 1995). In the wavefront analysis of normal eyes, the wavefront profile for astigmatic modes 4 and 6, as well as defocus mode 5, may be considered nominally circular (Webb, 1992), and the equivalent ophthalmic prescription may be computed from these modes. Treating these modes as circles W_4 , W_5 and W_6 represent the sags. The chord associated with each of these sags is the pupil diameter. Based on these assumptions and the geometry shown in Fig. 2.7, the dioptric curvature associated with each sag (W_4 , W_5 and W_6) may be computed by Eq. (2-24, 25 and 26) for modes 5, 4 and 6 respectively. Variable y is the pupil radius in the same unit used for W (meters).

$$M = 2W_5 / (y^2 + W_5^2) \quad (2-24)$$

$$J_{45} = 2W_4 / (y^2 + W_4^2) \quad (2-25)$$

$$J_0 = 2W_6 / (y^2 + W_6^2) \quad (2-26)$$

Variable M represents the mean spherical power, while J_{45} and J_0 are Jackson crossed cylinders with axes at 45/135 and 180/90 respectively.

3) Having been converted to diopters, the M, J_{45} and J_0 terms constitute the coefficients in a Cartesian Fourier decomposition of a spherocylindrical ophthalmic lens (Thibos, Wheeler, & Horner, 1997). The power derived from Zernike mode 4 (J_{45}) corresponds with sine term of the Fourier series and the mode 6 coefficient is used to compute the cosine term (J_0). The M, J_{45} and J_0 terms may be converted to the minus cylinder spectacle notation by the following formulas:

$$\text{Cylinder} = -2 (J_0^2 + J_{45}^2) \quad (2-27)$$

$$\text{Sphere} = M + \text{Cylinder} / 2 \quad (2-28)$$

$$\text{Axis} = \text{atan}(J_{45} / J_0) / 2 \quad (2-29)$$

In order to ensure that the computed axis agrees with clinical convention and is expressed as a positive angle, in degrees between 0 and 180, it may be necessary to add 90 or 180 degrees to the Axis value computed from Eq. (2-29) (Salmon & Horner, 1996). Table 2.2 organizes the conditional tests required to correctly change the value of Axis in Eq. (2-29) to the correct minus cylinder value. This can be summarized by the following computer pseudocode: “If $J_0 < 0$, add 90, else if $J_{45} < 0$, add 180, else no change.”

4) To express the refractive error in plus cylinder form, use Eq. (2-30) to compute the cylinder power. The Sphere and Axis values may be computed using Eqs. (2-28) and (2-29) as before, but the Axis value must be corrected according to the conditional tests shown in Table 2.3. This can be summarized by the following computer pseudocode: “If $J_0 > 0$, add 90, else if $J_{45} > 0$, add 180, else no change.”

$$\text{Cylinder} = 2 (J_0^2 + J_{45}^2) \quad (2-30)$$

TABLE 2.2 The value of Axis in Eq. (2-29) must be corrected according to the conditions summarized here, in order to obtain the correct minus cylinder axis.

Minus cylinder	If J_0 is ...		
	-	+	
If J_{45} is ...	-	axis = Axis + 90	axis = Axis + 180
	+	axis = Axis + 90	axis = Axis

TABLE 2.3 The value of Axis in Eq. (2-29) must be corrected according to the conditions summarized here, in order to obtain the correct plus cylinder axis.

Plus cylinder	If J_0 is ...		
	+	-	
If J_{45} is ...	+	axis = Axis + 90	axis = Axis + 180
	-	axis = Axis + 90	axis = Axis

An Excel spreadsheet that implements the Zernike-to-spectacle prescription conversion is included as Appendix A. This conversion will be used in Chapters 5 and 7 to compare clinically measured refractive errors with the corresponding Zernike coefficients.

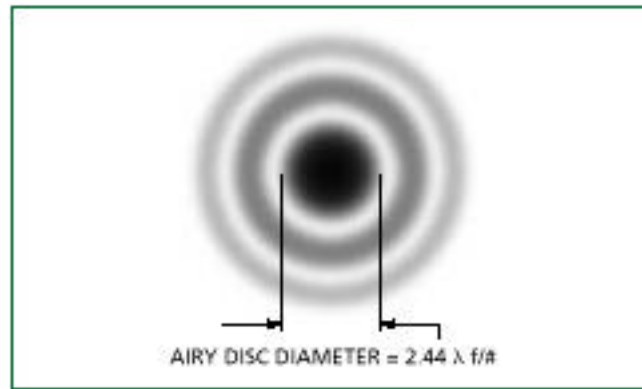


Figure 2.1

The Airy disc is the central intensity distribution in the focal plane of a diffraction limited optical system.

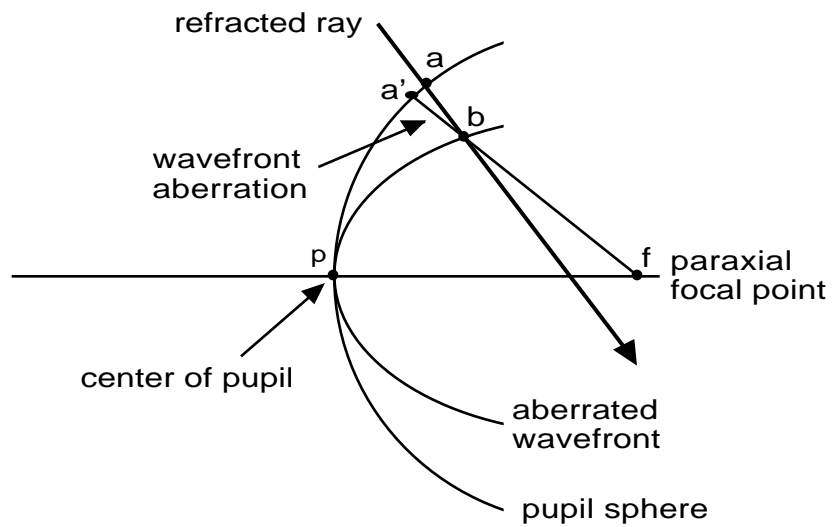


Figure 2.2

The wavefront aberration is the distance between the aberrated wavefront and the pupil sphere; that is, either distance ab or $a'b$, depending on the precise definition.

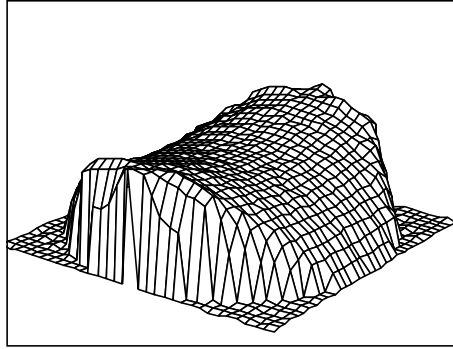


Figure 2.3

The wavefront aberration function may be represented by a surface centered in the exit pupil. Here astigmatism and spherical aberration form an asymmetric saddle shaped contour.

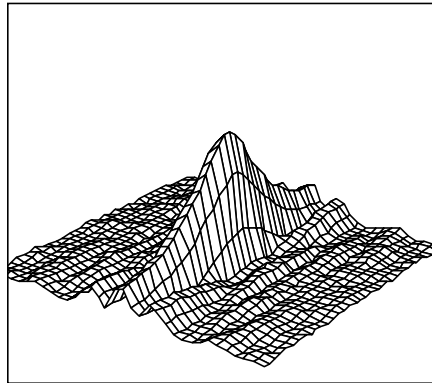


Figure 2.4

Surface plot of an MTF for a theoretical cornea with astigmatism and spherical aberration. This corresponds with the wavefront shown in Fig. 2.3.

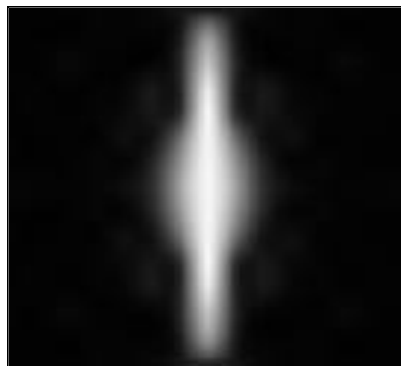


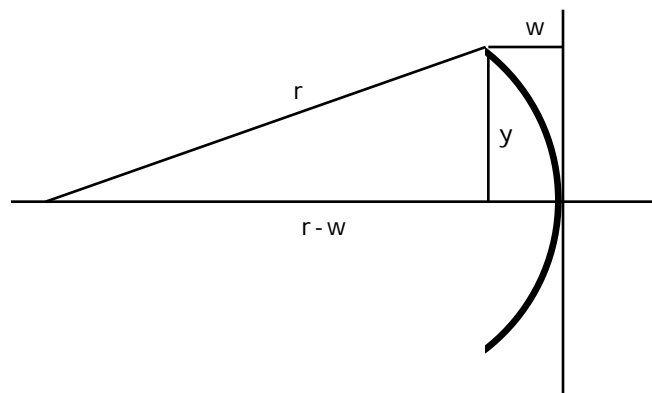
Figure 2.5

Point spread function for a theoretical toric cornea at the “circle” of least confusion. This corresponds with the wavefront of Fig 2.3 and MTF of Fig. 2.4.



Figure 2.6

Convolving the scene on the left with the PSF of Fig. 2.5 yields the blurred image on the right and simulates the effect of corneal astigmatism and spherical aberration. Deconvolution would recover the scene (left) from the aberrated image (right).



$$\begin{aligned}
 r^2 &= (r-w)^2 + y^2 \\
 r^2 &= r^2 - 2rw + w^2 + y^2 \\
 2rw &= w^2 + y^2 \\
 r &= \frac{(w^2 + y^2)}{2w}
 \end{aligned}$$

Figure 2.7

Geometry used to find the radius of curvature (r) of a circle based on measurements of its sag (w) at a distance y from the apex. If the r is measured in meters, the inverse of r is the curvature in diopters (D). This is a familiar problem in ophthalmic optics.